Pyrolysed cellulose nanofibrils and dandelion pappus in supercapacitor application

Juhani Virtanen · Arno Pammo · Jari Keskinen · Essi Sarlin · Sampo Tuukkanen

Abstract Dandelion pappus and wood based nanocellulose fibrils were combined to form films that were subsequently pyrolyzed under low-pressure conditions in a carbon monoxide (CO) rich atmosphere to make supercapacitorelectrode material. The electrodes were prepared from these materials and pyrolysed under low-pressure conditions in a carbon monoxide-rich atmosphere. The electrode materials and assembled supercapacitors were electrically and structurally characterized. The assembled six supercapacitors showed specific capacitances per electrode ranging from 1 to 6 F/g and surface resistance of pyrolyzed electrodes ranging from 30 to 170 Ω/□. Finally, equivalent series resistance and leakage current measurements were conducted for three samples, resulting values from 125 to 500 Ω and from 0.5 to 5.5 μA, respectively.

J. Virtanen · A. Pammo · S. Tuukkanen (✉)
Biomeditech institute and Faculty of Biomedical Sciences and Engineering, Tampere University of Technology, P.O. Box 692, 33101 Tampere, Finland
e mail: sampo.tuukkanen@tut.fi

J. Keskinen
Laboratory of Electronics and Communications Engineering, Tampere University of Technology, P.O. Box 692, 33101 Tampere, Finland

E. Sarlin
Laboratory of Materials Science, Tampere University of Technology, P.O. Box 589, 33101 Tampere, Finland

Keywords Supercapacitor · Nanocellulose · Dandelion · Pyrolysis

Introduction

Because of global challenges such as ever-increasing misuse of natural resources, deterioration of environment, energy crisis, and global warming, there is a huge push towards bioeconomy. Bioeconomy comprises the production of renewable biological resources and their conversion into food, feed, bio-based products, and bioenergy. One step towards bioeconomy is the fabrication of electronics and energy storage components from renewable biomaterials.

Nanocellulose materials (Moon et al. 2011), such as cellulosic nanofibrils and cellulose nanocrystals, are interesting renewable bio-based nanomaterials with potential applications in different fields. The nanoscale dimensions and strong ability to form entangled porous networks make nanocelluloses suitable materials for fabrication of lightweight membranes, films, and nanopapers, all of which can be processed in aqueous media. Processing in aqueous media allows low-cost and high-throughput manufacturing of functional devices for applications such as power storage (Lehtimäki et al. 2015), touch sensing (Vuorinen et al. 2014), and optics (Isoniemi et al. 2015). On the other hand, the combination of nanocellulose with solution processable carbon-based nanomaterials, such as carbon nanotubes or graphene, enables fabrication of

flexible and disposable devices, including supercapacitors (Tuukkanen et al. 2014; Torvinen et al. 2015; Lehtimäki et al. 2014). Supercapacitors, also known as electrochemical double-layer capacitors (EDLC), are potential energy storage devices that are safe and disposable (Pettersson et al. 2014; Keskinen et al. 2016) low cost electronics for personal medical devices or Internet-of-Things applications. Quite a few reports in the recent literature reveal the raising interest towards taking advantages of nanocellulose in energy storage devices in different ways (Erlandsson et al. 2016; Wang et al. 2015, 2016; Zolin et al. 2016).

Pyrolysis is generally used for carbonization of biomaterials to produce conducting and porous structures, which are optimal electrode materials for supercapacitors. Carbonized nanocellulose has been recently used as a supercapacitor electrode (Zu et al. 2016; Wu et al. 2013). In this study a carbon monoxide rich atmosphere was targeted to promote the carbonisation and graphitisation of the prepared electrodes as the natural gasification of the cellulose biomass produces the desired carbon monoxide (Wu et al. 2013). Under these conditions, graphitization takes place through Boudouard reaction. The graphitization of the samples is essential as the capacitor assembly does not contain any specific current collector structure but the active electrode also acts as a current collector. The conductivity of nanocellulose and dandelion pappus is negligible, and thus conductivity improvement is essential to obtain functional supercapacitors.

Taraxacum species, or more commonly dandelions, are plants often regarded as weeds. They grow well in very different climates and environments (United States Department of Agriculture). Dandelions have some intriguing features making them usable as raw material. For instance, *Taraxacum kok-saghyz* (Russian dandelion) has been used to produce natural rubber (van Beilen and Poirier 2007; Dzuck 2015; Schmidt et al. 2010). Dandelions are also non-toxic and edible herbs, e.g. *Taraxacum officiale* contains high amounts of vitamin A, iron, and calcium (United States Department of Agriculture, Agricultural Research Service 2016; Ward 1936).

In this study, we have prepared bio-based composite films from cellulose nanofibers and dandelion pappus. The films then undergo high-temperature pyrolysis to produce electrically conducting and highly porous electrodes. Incorporation of dandelion pappus as a natural source of nearly pure cellulose potentially increased the structural strength of pyrolysed films due to elongated shape of fibrous pappus. These carbonized films are subsequently assembled into supercapacitor configuration and electrochemically characterized. To our knowledge, this is the first study exploring the possibilities of dandelion as a bio-based structural component in electronics application.

Materials and methods

Nanocellulose

Cellulose nanofibrils (CNFs) used in the experiments were made by processing bleached sulphite birch fibers suspended in water through a Masuko grinder using three consecutive passes. This was followed by homogenization of six passes at 2000 bar pressure using M110P microfluidizer (Microfluidics Corp., Newton, MA, USA) equipped with 200 and 100 μm chambers. CNFs was dispersed in aqueous medium forming a highly viscous hydrogel as shown in Fig. 1a. Dry weight contents of used CNF batches were 1.35 and 1.69 wt% for samples SC-1 to SC-3 and SC-4 to SC-6, respectively. The mechanically fibrillated CNF used here is a mixture of different size fibrils from nano- to microscale and also contains some residual larger fibers which can be observed in SEM images (see Fig. 1b) of CNF films (Rajala et al. 2016). Österberg et al. have found that fibrils in similar CNF gel are many micrometers long, and the diameter of thicker fibrils is in the 50−100 nm range, whereas the majority of the fibrils are in the 5−20 nm diameter range (Österberg et al. 2013).

Dandelion pappus

Dandelion pappus was separated from the seeds by placing them in a jar with metallic nuts. The jar was shaken by hand for 5 min, which resulted in the detachment of the seeds from the pappus. The pappus gained a resemblance to a cotton ball (see Fig. 1c), while the seeds accumulated on the bottom of the jar. Based on the optical microscope analysis, the average length of used pappus fibers was about 5 mm, and their diameter was in the range of 15 20 μm (see Fig. 1d).

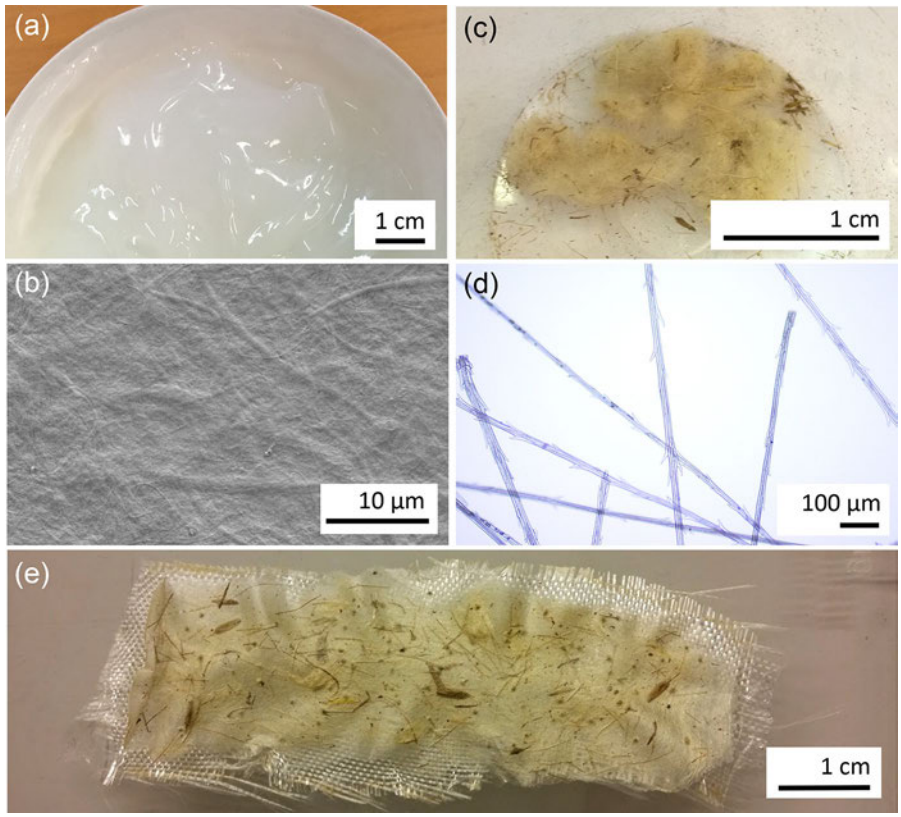

Fig. 1 Photographs of **a** CNF (cellulose nanofibril) gel, **b** SEM image of CNF film, **c** dandelion pappus fibers, **d** microscope image of dandelion pappus fibers, and **e** CNF/dandelion mixture deposited on glass fiber substrate (*before* pyrolysis)

Composite film preparation

CNF gel and the dandelion pappus were mixed together and stirred until a homogeneous mixture was formed. In a typical experiment, about 15 mg of dandelion pappus was mixed with about 5 g of CNF gel. The dry CNF to dandelion pappus mass ratio was 4:1 in the samples SC-1 to SC-3, and 5:1 in the samples SC-4 to SC-6. The mass ratio was changed to evaluate its effect to the specific capacitance. The gel mixture was then applied to a piece of fiberglass, and the film was subsequently dried on a hotplate. Fiberglass provided structural firmness to the sample making it easier to handle. Fiberglass was chosen as a substrate material because the CNF/pappus mixture did not stick to it, enabling its facile removal after pyrolysis in order to assemble the supercapacitors. Otherwise the sample might crack and flake during pyrolysis. Fiberglass also withstands well high temperatures used in the pyrolysis. The CNF/dandelion mixture deposited on a glass fiber substrate is shown in Fig. 1e. To enable the film deposition by solution processing technique, CNF gel acted as a carrier material for dandelion. To obtain a reference sample, pyrolysis was performed also for bare CNF films, but afterward, the pyrolysis samples became so brittle that a supercapacitor assembly was not possible.

Pyrolysis

Pyrolysis of the prepared samples was conducted in tube furnace (ST-1200RGX). The tube furnace pyrolysis setup was carried out in low-pressure conditions with continuous suction of a vacuum pump (1-stage vacuum pump VE-115). The pressure level during the pyrolysis was estimated to be 5 Pa (0.05 mbar).

During pyrolysis, a temperature profile program (see Fig. 2a) was run in the furnace, and after the program a natural cooling of the furnace and samples took place. After cooling, the samples (see Fig. 2b) were further processed for measurement.

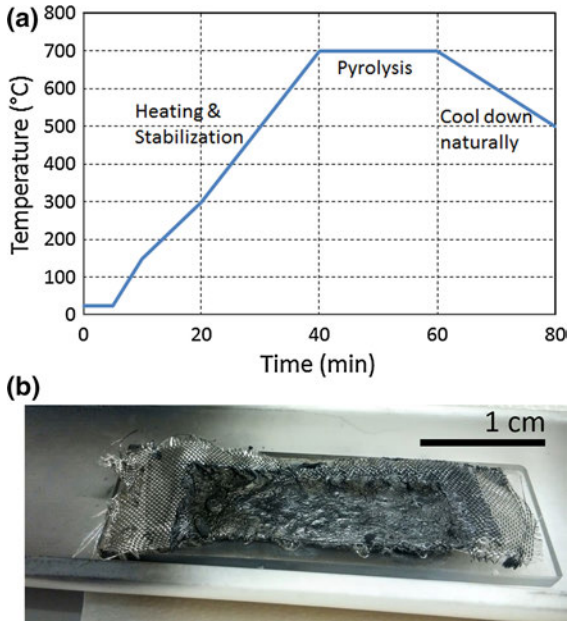

Fig. 2 **a** The tube furnace temperature profile during the pyrolysis process. **b** An example of pyrolyzed nanocellulose dandelion film on glass fiber substrate

Dried samples were placed between paper and quartz plates on a ceramic tray. The quartz plates ensured that the samples stayed straight and prevented them from curling up. Paper worked as a cushion between the quartz and the sample. There was some variation in the thickness, but an average value of about 300 μm was obtained with a micrometer gauge.

Supercapacitor assembly

The pyrolysed CNF/dandelion composite electrode was cut to suitable size pieces using scalpel and scissors, and the pieces were placed on two 25 mm × 10 mm × 3 mm quartz plates using double-sided adhesive film. These two smaller electrodes were piled up perpendicularly as described in Fig. 3a. Contact area was thus 100 mm (Lehtimäki et al. 2015). A paper separator was used along with 1 M NaCl solution as electrolyte. A photograph of 3D-printed measurement jig for supercapacitor assembly is shown in Fig. 3b and its closing procedure schematically in Fig. 3c.

The pyrolysed CNF/dandelion composite electrodes were studied by scanning electron microscope (SEM, Zeiss ULTRAplus). A thin carbon layer was evaporated on top of the electrode to ensure its

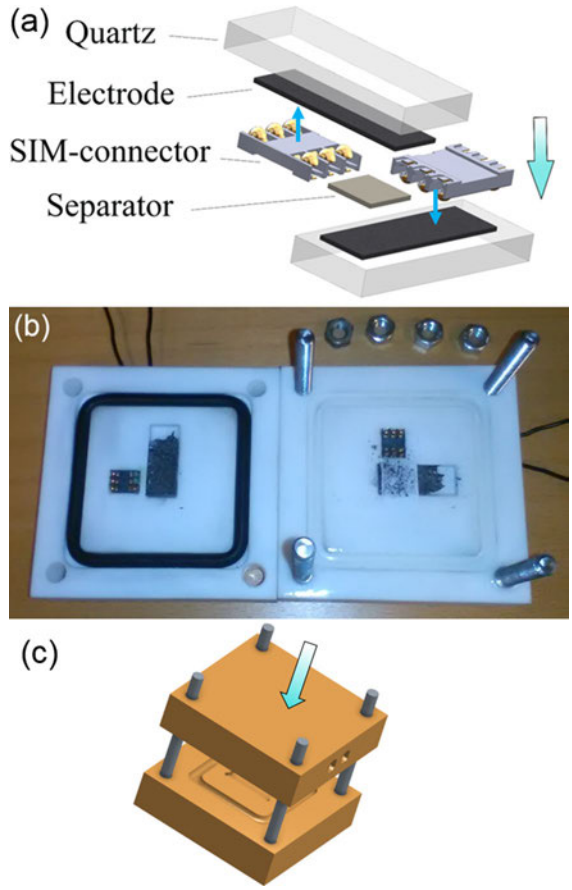

Fig. 3 **a** Schematic view of the supercapacitor assembly. **b** An opened measurement jig with assembled electrodes on quartz plates and a separator paper. **c** CAD picture of jig while closing it

electrical conductivity in the microscope. Elemental analysis was done with energy dispersive X-ray spectroscopy (EDS) with INCAx-act silicon-drift detector from Oxford Instruments.

Electrical measurements

The electrical measurements were performed with an IviumStat potentiostat (Ivium Technologies B.V.) and Maccor 4300 Test Station. The IviumSstat was used to perform CV-curves and surface resistance measurements while the Maccor was used to carry out capacitance, equivalent series resistance (ESR), leakage current, and efficiency measurements. Because of the nature of the samples, a 2-point measurement configuration was used. This was justified because the contact resistance is expected to be much smaller than

the pyrolysed film resistance. Also, the resistivity of dry electrodes after pyrolysis was measured using an IviumStat potentiostat in 2-point measurement. Sheet resistance of electrodes was measured from a square area using gold plated SIM-connector contacts (MOLEX SD-47017-002, Molex incorporated), which can be seen in Fig. 3a. The samples were attached to a fixture and the electrical connection to the samples was arranged with custom made gold plated contact probes.

Reference measurements for the measurement system and jig assembly

Reference measurements were carried out to verify the supercapacitor (EDLC) jig assembly capacitance and contact resistances. This was made in order to ensure that the jig assembly did not contribute to or falsify the electrical measurements of assembled supercapacitors. The supercapacitor measurement jig and the pyrolyzed electrodes on quartz are shown in Fig. 3. The 3D printed plastic measurement jig was purchased from Shapeways, Inc. The electrical connections to the pyrolysed samples were arranged through SIM-connectors with 3D vertical connections were connected electrically. Both 2-point and 4-point measurements could be arranged to the samples with this setup. The jig was sealed with a nitrile rubber gasket and a layer of polydimethylsiloxane (PDMS) film in order to avoid electrolyte loss during the measurement. The bottom and top jig assemblies were secured together during the measurements with four threaded bars and nuts.

The reference sample electrodes were prepared on the same quartz glass plates by coating them with Acheson Electrodag PF407-C carbon ink and curing the ink for 20 min at 120 °C. The cured layer thickness of the ink was approximately 20 µm. This carbon ink was used in order to demonstrate the functionality of measurement setup using a well-known carbon-based electrode material, which is optimised for conductor application and, therefore, has a small surface area that contributes to a reference device capacitance.

The same separator material and electrolyte as with the pyrolysed samples were used with the graphite ink reference capacitor assembly. The CV curve measurements can be seen in Fig. 4. From the measurement

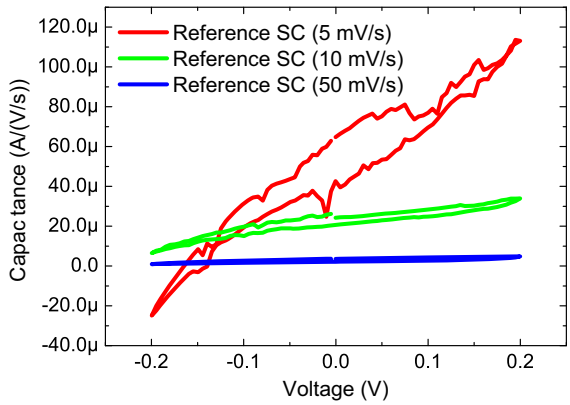

Fig. 4 CV curves from a reference supercapacitor having carbon ink electrodes assembled to the jig for setup test measurements

results it can be concluded that the jig assembly contribution to the capacitance of the pyrolysed sample measurements is several orders of magnitude smaller than what was measured from the pyrolysed samples even with the conductive carbon ink electrode capacitor in place. The calculated capacitance values of this jig capacitance measurement with 5, 10, and 50 mV/s setup were 12.79, 3.30, and 1.25 µF, respectively. Thus, the assembly contributes a negligible error to the actual measurement results.

Constant current capacitance, ESR, and leakage current definition

Constant current capacitance, ESR, and leakage current measurements were performed for samples 3, 4, and 6 with a Maccor 4300 test station. The actual measurement was started with three constant current charge discharge cycles. Each cycle was conducted using 20 µA charging and discharging current in the potential range 0 0.2 V. After the third cycle the potential was kept constant at 0.2 V for 30 min. The ESR value was calculated from the IR-drop after this holding period. Capacitance was defined between 0.16 and 0.08 V during constant current discharge. After measuring the capacitance the supercapacitor was charged to 0.2 V and kept at this potential for 1 h. Leakage current was defined to be the current needed to keep the voltage constant in the end of this 1 h period. Charge and energy efficiency values were calculated from the third charge discharge cycle in the beginning of the measurement procedure.

Results and discussion

Scanning electron microscopy and elemental analysis

Scanning electron microscope (SEM) analysis including energy dispersive X-ray spectroscopy (EDS) was performed for pyrolysed electrodes from supercapacitors SC-5 and SC-6 (see Fig. 5). From SEM images one can see that even after pyrolysis dandelion pappus-shaped objects remain when comparing to the recent literature showing dandelion structures (Meng et al. 2014; Hale et al. 2010). As we expected in this study, the longitudinal objects resulting from pappus fibers appear with diameter similar to that prior the pyrolysis (see Fig. 1d). The addition of pappus fibers into the CNF gel increased the robustness of pyrolysed electrodes, which is most likely related to remaining network of carbonised pappus structures. We expected that after the pyrolysis pappus fibres act as wires to carry electrical current in longitudinal direction better than carbonized nanocellulose matrix around them.

From the EDS results (Table 1) one can see that after pyrolysis there is about 90% of carbon in the sample electrodes. However, approximately 10% oxygen also remained in the samples. The presence of a rather high amount of the oxygen left in the samples suggests that graphite oxide or graphene oxide is present in the samples. This, however, was not verified in any means in this study. Even though the EDS analysis was performed after the electrical measurements of the EDLC and the electrodes were washed with deionised water before the SEM-analysis, some residues of Na and Cl are present most likely resulting from the NaCl electrolyte. The amount of other atomic constituents was very small.

Electrode fabrication and surface resistance measurements

Current voltage (IV) characteristics of dry pyrolysed electrodes were measured using the potentiostat. In

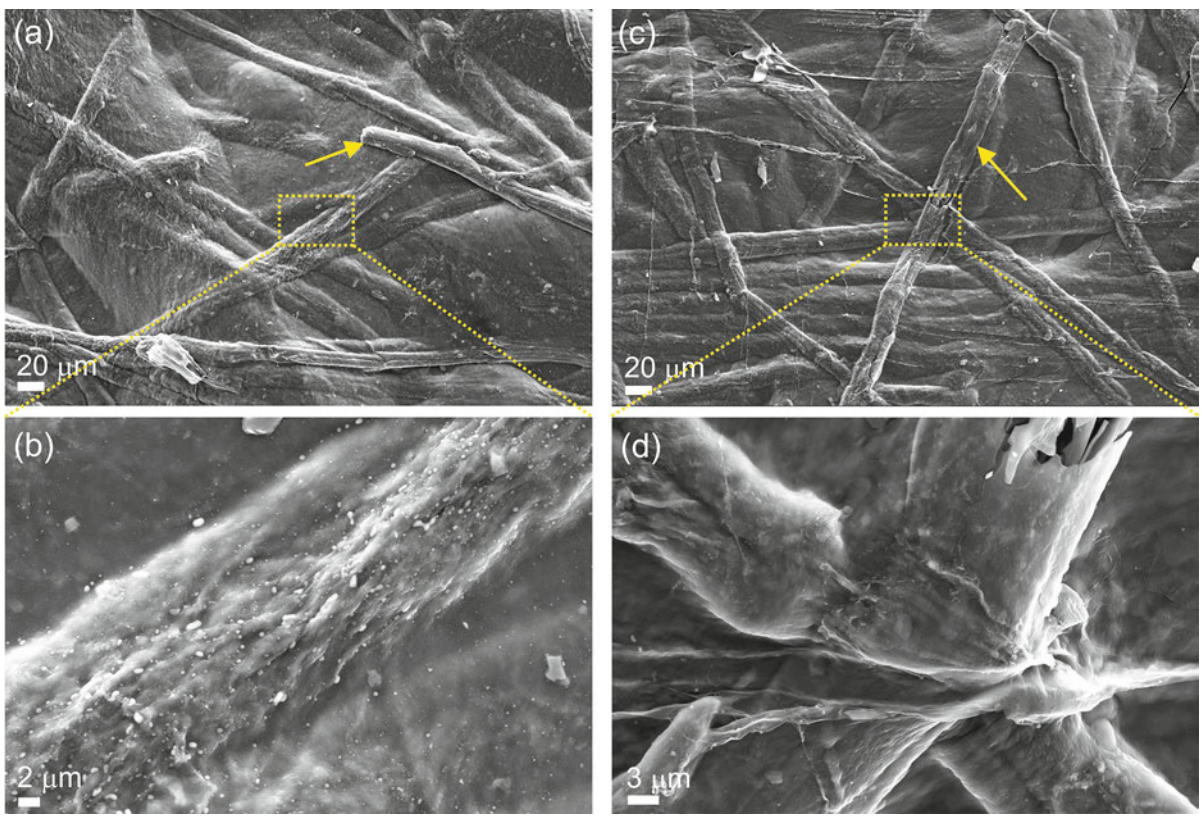

Fig. 5 Scanning electron microscope (SEM) images and energy dispersive X ray spectroscopy (EDS) analysis for electrodes from samples SC 5 (**a** **b**) and SC 6 (**c** **d**). The *arrows* are pointing to the dandelion pappus fibers after pyrolysis

Table 1 Elemental analysis for electrodes from samples SC 5 and SC 6 showing mainly carbon and oxygen and traces of other elements

Weight %	C	O	F	Na	Mg	Al	Si	P	Cl	K	Ca
SC 5	84	11	<1	1	<1	<1	<1	<1	2	<1	<1
SC 6	86	10	<1	1	<1	<1	<1	<1	1	<1	<1

Fig. 6, there is one curve presented for each supercapacitor, because the two electrodes used for each SC were nominally similar. Table 2 shows the electrode masses before and after pyrolysis, as well as sheet resistance R_S for each pair of electrodes used in the assembly of each supercapacitor. The reason for using the voltage sweep for surface resistance measurements was to ensure an ohmic nature (linear curves) of the electrodes and the contacts.

The mass loss is different between the first three and the latter three samples. This was due to larger surface-to-volume ratio in the first three samples, causing them to dry more thoroughly before pyrolysis. The large mass loss in Table 2 is thus largely due to water evaporation.

CV-measurements

Figure 7 shows the cyclic voltammetry (CV) curves for six assembled supercapacitors using three different sweep rates (5, 10, and 50 mV/s). To make CV curves with different speeds comparable, y-axis is plotted in principal units of capacitance obtained by dividing unit of current (A) by the unit of sweep rate (V/s). In these curves, a measured current charging and discharging capacitor is shown as a function of voltage when the capacitor assembly is charged and discharged at a constant voltage sweep. The voltage sweep range was selected to be from −0.2 0.2 V to reveal the symmetry of the capacitor structure, thereby forcing both polarity ions to travel to both electrodes. The low voltage range is also used to ensure that faradaic effects are not present during the measurements. The CV-measurements were carried out with a non-hermetic capacitor structure, which was exposed to drying of the electrolyte during the measurement. Because of the water vapor leakage from the jig due to the electrolyte evaporation, the minimisation of sweeping time was important. Furthermore, the long-term cycling tests were not carried out as the capacitor structure in the jig assembly was not capable of holding water for long periods of time. Without this property the capacitor assembly electrolyte dries and prevents the structure to function as an EDLC.

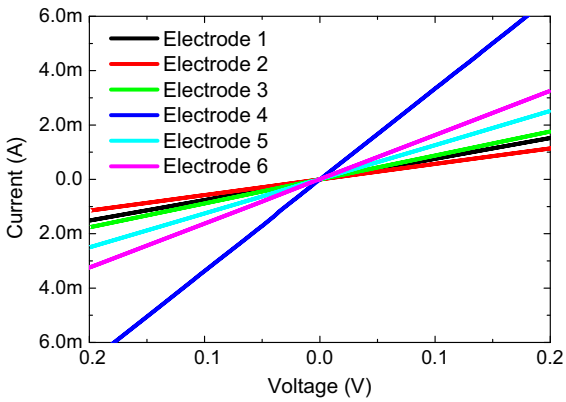

Fig. 6 Current voltage (IV) curves for dry electrodes after pyrolysis. The curves were captured using 50 mV/s scan rate. IV curves are given for six electrodes, which each was used for assembly of different supercapacitors. Two nominally identical electrodes were used for assembly of each supercapacitor

Calculated capacitance

The capacitances of assembled supercapacitors were calculated from the CV curves presented in Fig. 7. Because of the symmetric nature of the capacitors, the capacitances were calculated from captured charge and voltage range ($C = Q/V$) by integrating the current over both the charge and discharge cycles and dividing the resulted integral value by 2. This way we neglect the contributions from possible Faradaic reactions and the nonsymmetry of the assembled EDLC structure. Table 3 shows the capacitance in millifarads (mF) calculated for each sample with different voltage sweep rates.

Galvanostatic charge discharge measurements

The results of galvanostatic charge discharge measurements performed using a Maccor are shown in Table 4. Examples of measured GCD curves for

Table 2 Electrode mass before and after pyrolysis, mass loss, and sheet resistances obtained from the IV curves shown in Fig. 6

Samples	Mass of two electrodes before pyrolysis (mg)	Mass of two electrodes after pyrolysis (mg)	Mass loss pyrolysis (%)	R_S and standard deviations (Ω/□)
SC 1	85.0	13.0	84.7	131 ± 3
SC 2	89.1	13.5	84.8	174 ± 4
SC 3	156	12.1	92.2	114 ± 1
SC 4	296	16.0	94.6	29.4 ± 0.4
SC 5	314	16.7	94.7	82 ± 2
SC 6	278	12.1	95.6	62.3 ± 1.5

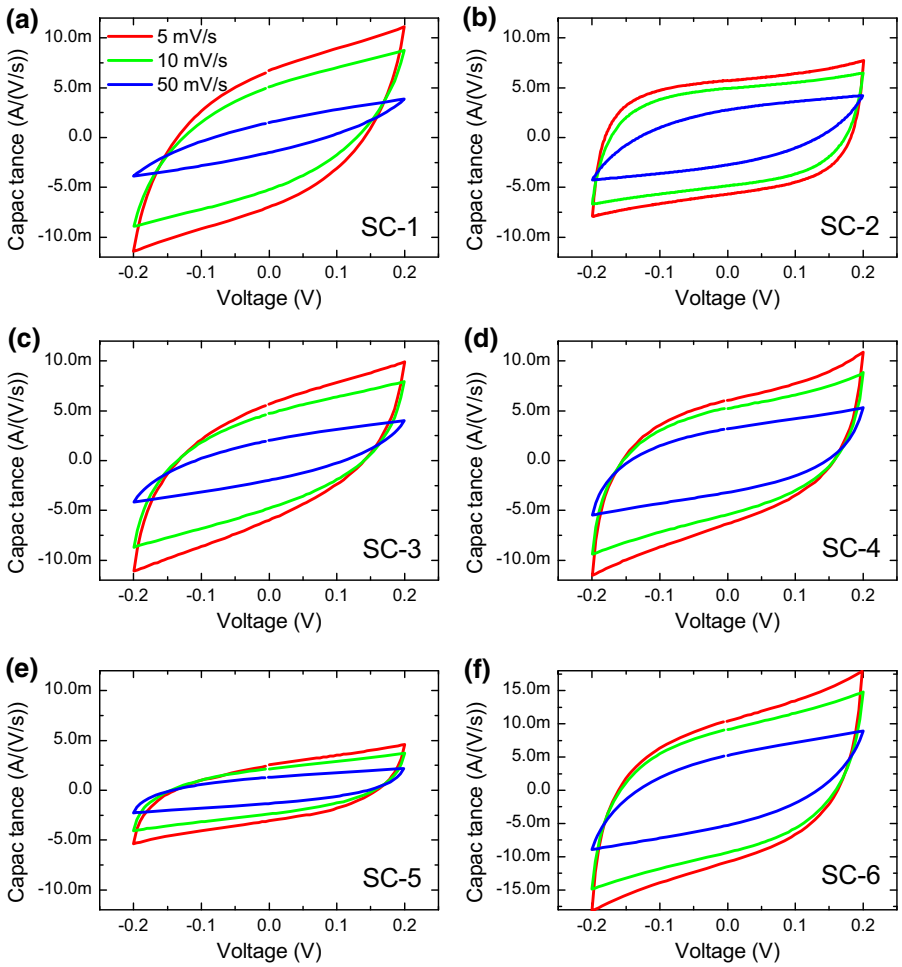

Fig. 7 **a** **f** Cyclic voltammetry (CV) curves for six assembled supercapacitors (SC 1 to SC 6) with different scan rates. The *y axes* are plotted as current per scan rate resulting qualitatively the unit of capacitance

supercapacitor SC-6 are shown in Fig. 8. These can be compared with the capacitance values calculated for the IviumStat CV-measurements above. The capacitance values measured with both devices are at same range with reasonable accuracy. High series resistance of 500 Ω with sample SC-4 may contribute

Table 3 The supercapacitor capacitances from the CV curves and calculated specific capacitances per electrode

Samples	C (mF) at 5 mV/s	C (mF) at 10 mV/s	C (mF) at 50 mV/s	Specific capacitance C_{sp} per electrode (F/g) at 5 mV/s
SC 1	11.0	8.07	2.25	3.39
SC 2	10.3	8.47	4.12	3.06
SC 3	9.78	7.90	3.12	3.25
SC 4	11.1	9.33	5.35	2.77
SC 5	4.86	3.93	2.22	1.16
SC 6	19.1	16.2	8.41	6.27

to the difference in capacitance values. Because of slow charging and discharging with 20 µA, the leakage current has a remarkable effect on the efficiency values. For sample SC-4, which had the lowest leakage current, the energy efficiency was measured to be 64% and the charge efficiency 96%. Since SC-6 has considerably larger capacitance than SC-5 and relatively smaller leakage current, it shows higher efficiency than SC-5. Also, the lower ESR of SC-6 improves its efficiency compared to SC-5. The variation of the specific capacitances in the samples may be contributed by the dandelion pappus because the material was gathered directly from a green yard, and the different properties of the soil in the plant growth or other atmospheric contaminations might have affected the outcome of the pyrolysed samples.

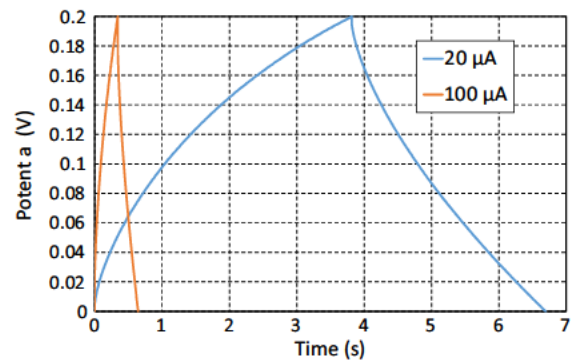

Fig. 8 Galvanostatic charge discharge curves from the super capacitor SC 6

Conclusion

Mechanically fibrillated nanocellulose gel mixed with decollated dandelion pappus was carbonized by pyrolysis and used as supercapacitor electrode material without the need for a separate current collector. To our knowledge, we show here for the first time that this type of natural organic material and their simple processing yields functional nanoscale materials that are promising for high end product applications. It was found that carbon monoxide (CO)-rich atmosphere in the pyrolysis process results in functional supercapacitor electrode material.

The preparation and assembly of biomaterial films for pyrolysis was found to be delicate, and thus there were relatively large variations in the performance of fabricated six supercapacitors. However, the sample fabrication process improved during the work progress from SC-1 to SC-6 and showed a learning curve yielding better performance for the latter devices. The performance of supercapacitors fabricated in this work is comparable to our previous study where solution processed ink from carbon nanotubes and hemicellulose was used (Lehtimäki et al. 2014). In comparison,

Table 4 The electrical properties for SC 4 to SC 6 from capacitance, ESR, leakage current and efficiency measurements

Sample	ESR (Ω)	Capacitance (mF)	Leakage current (µA)	N (E)%	N (Q)%
SC 4	500	3.5	0.53	64	96
SC 5	250	8.3	3.75	32	57
SC 6	125	20.5	5.5	46	76

the nanocellulose and dandelion materials used in this study are significantly cheaper and natural organic biomaterials.

To conclude, active electrode material for supercapacitors was prepared using high temperature pyrolysis of solution processed films of cellulose nanofibril and dandelion pappus mixture. Specific capacitances over 6 F/g were obtained in this work. The results suggest that this type of natural organic material has potential as a green, safe, and low-cost supercapacitor material.

Author contributions JV and AP has fabricated the composite electrodes, performed the high temperature pyrolysis, and performed the electrical measurements using Ivium potentiostat, as well as analysed the data. JK has performed the electrical measurements with Maccor equipment. JV, AP and ST has written the most of the manuscript. ES has performed the SEM and EDS analysis. All authors commented the manuscript and gave their approval to the final version of the manuscript.

Compliance with ethical standards

Conflict of interest The authors declare no competing financial interest.

References

Dzuck S (2015) Fraunhofer Gesellschaft company press release: natural rubber from dandelions. Research news special issue. 8.6.2015. https://www.fraunhofer.de/en/press/research news/2015/June/natural rubber from dandelions.html

Erlandsson J, Durán VL, Granberg H, Sandberg M, Larsson PA, Wågberg L (2016) Macro and mesoporous nanocellulose beads for use in energy storage devices. Appl Mater Today 5:246 254. doi:10.1016/j.apmt.2016.09.008

Hale AN, Imfeld SM, Hart CE, Gribbins KM, Yoder JA, Collier MH (2010) Reduced seed germination after pappus removal in the North American dandelion (Taraxacum officinale; Asteraceae). Weed Sci 58(4):420 425. doi:10.1614/WS D 10 00036.1

Isoniemi T, Tuukkanen S, Cameron DC, Simonen J, Toppari JJ (2015) Measuring optical anisotropy in poly(3,4 ethylene dioxythiophene):poly(styrene sulfonate) films with added graphene. Org Electron 25:317 323. doi:10.1016/j.orgel.2015.06.037

Keskinen J, Lehtimäki S, Dastpak A, Tuukkanen S, Flyktman T, Kraft T, Railanmaa A, Lupo D (2016) Architectural modifications for flexible supercapacitor performance optimization. Electron Mater Lett 12:795 803. doi:10.1007/s13391 016 6141 y

Lehtimäki S, Suominen M, Damlin P, Tuukkanen S, Kvarnström C, Lupo D (2015) Preparation of supercapacitors on flexible substrates with electrodeposited PEDOT/graphene composites. ACS Appl Mater Interface 7(40):22137 22147. doi:10.1021/acsami.5b05937

Lehtimäki S, Tuukkanen S, Pörhönen J, Moilanen P, Virtanen J, Honkanen M, Lupo D (2014) Low cost, solution processable carbon nanotube supercapacitors and their characterization. Appl Phys A 117(3):1329 1334. doi:10.1007/s00339 014 8547 4

Meng Q, Wang Q, Liu H, Jiang L (2014) A bio inspired flexible fiber array with an open radial geometry for highly efficient liquid transfer. NPG Asia Mater 6(9):e125. doi:10.1038/am.2014.70

Moon RJ, Martini A, Nairn J, Simonsen J, Youngblood J (2011) Cellulose nanomaterials review: structure properties and nanocomposites. Chem Soc Rev 40(7):3941 3994. doi:10.1039/C0CS00108B

Österberg M, Vartiainen J, Lucenius J, Hippi U, Seppälä J, Serimaa R, Laine J (2013) A fast method to produce strong NFC films as a platform for barrier and functional materials. ACS Appl Mater Interface 5(11):4640 4647. doi:10.1021/am401046x

Pettersson F, Keskinen J, Remonen T, von Hertzen L, Jansson E, Tappura K, Zhang Y, Wilén C E, Österbacka R (2014) Printed environmentally friendly supercapacitors with ionic liquid electrolytes on paper. J Power Sources 271:298 304. doi:10.1016/j.jpowsour.2014.08.020

Rajala S, Siponkoski T, Sarlin E, Mettänen M, Vuoriluoto M, Pammo A, Juuti J, Rojas OJ, Franssila S, Tuukkanen S (2016) Cellulose nanofibril film as a piezoelectric sensor material. ACS Appl Mater Interface 8(24):15607 15614. doi:10.1021/acsami.6b03597

Schmidt T, Lenders M, Hillebrand A, van Deenen N, Munt O, Reichelt R, Eisenreich W, Fischer R, Prüfer D, Gronover C (2010) Characterization of rubber particles and rubber chain elongation in Taraxacum koksaghyz. BMC Biochem. doi:10.1186/1471 2091 11 11

Torvinen K, Lehtimäki S, Keränen JT, Sievänen J, Vartiainen J, Hellén E, Lupo D, Tuukkanen S (2015) Pigment cellulose nanofibril composite and its application as a separator substrate in printed supercapacitors. Electron Mater Lett 11(6):1040 1047. doi:10.1007/s13391 015 5195 6

Tuukkanen S, Lehtimaki S, Jahangir F, Eskelinen A P, Lupo D, Franssila S (2014). Printable and disposable supercapacitor from nanocellulose and carbon nanotubes. In Proceedings of the 5th electronics system integration technology conference (ESTC). IEEE, pp 1 6. DOI: 10.1109/ESTC.2014.6962740

United States Department of Agriculture, Agricultural Research Service (2016): full report (all nutrients), 11207, Dandelion greens, raw. Accessible at https://ndb.nal.usda.gov/ndb/foods/show/2960?fgcd=&manu=&lfacet=&format=Full&count=&max=50&offset=&sort=default&order=asc&qlookup=11207&ds=

van Beilen J, Poirier Y (2007) Establishment of new crops for the production of natural rubber. Trends Biotechnol 25(11):522 529. doi:10.1016/j.tibtech.2007.08.009

Vuorinen T, Zakrzewski M, Rajala S, Lupo D, Vanhala J, Palovuori K, Tuukkanen S (2014) Printable, transparent, and flexible touch panels working in sunlight and moist environments. Adv Funct Mater 24(40):6340 6347. doi:10.1002/adfm.201401140

Wang Z, Carlsson DO, Tammela P, Hua K, Zhang P, Nyholm L, Strømme M (2015) Surface modified nanocellulose fibers

yield conducting polymer based flexible supercapacitors with enhanced capacitances. ACS Nano 9(7):7563 7571. doi:10.1021/acsnano.5b02846

Wang Z, Tammela P, Huo J, Zhang P, Strømme M, Nyholm L (2016) Solution processed poly(3,4 ethylenedioxythio phene) nanocomposite paper electrodes for high capaci tance flexible supercapacitors. J Mater Chem A 4:1714 1722. doi:10.1039/C5TA10122K

Ward H. Herbal Manual. The C. W. Daniel Company Ltd, London. 1936. ISBN 10: 0852430086

Wu C, Wang Z, Huang J, Williams PT (2013a) Pyrolysis/gasi fication of cellulose, hemicellulose and lignin for hydrogen production in the presence of various nickel based cata lysts. Fuel 106:697 706. doi:10.1016/j.fuel.2012.10.064

Wu XL, Wen T, Guo HL, Yang S, Wang X, Xu AW (2013b) Biomass derived sponge like carbonaceous hydrogels and aerogels for supercapacitors. ACS Nano 7(4):3589 3597. doi:10.1021/nn400566d

Zolin L, Nair JR, Beneventi D, Bella F, Destro M, Jagdale P, Cannavaroe I, Tagliaferroe A, Chaussy D, Geobaldoe F, Gerbaldi C (2016) A simple route toward next gen green energy storage concept by nanofibres based self support ing electrodes and a solid polymeric design. Carbon 107:811 822. doi:10.1016/j.carbon.2016.06.076

Zu G, Shen J, Zou L, Wang F, Wang X, Zhang Y, Yao X (2016) Nanocellulose derived highly porous carbon aerogels for supercapacitors. Carbon 99:203 211. doi:10.1016/j.carbon.2015.11.079